7. Final conclusions

After a general introduction in **chapter 1**, the results discussed in chapters 2 to 6 encompass basic questions about sub-seismic structures and deformational processes and their relation to large-scale structures.

In **chapter 2** we present results from interpretation of a 3D seismic data set, located within the NW German sedimentary basin. We focused on the development of faults, the timing of deformation, the amount of displacement during multiphase deformation, strain partitioning, and the interaction between salt movement and faulting. We recognised the central fault zone of the study area to be the Aller-lineament, an important NW-trending fault zone within the superimposed Central European Basin System. From structural and sedimentological interpretations we derived the following evolution: (1) E-W extension during Permian rifting, (2) N-S extension within cover sediments, and E-W transtension affecting both basement and cover, contemporaneously during Late Triassic and Jurassic, (3) regional subsidence of the Lower Saxony Basin during Late Jurassic/Early Cretaceous, (4) N-S compression within cover sediments, and E-W transpression affecting both basement and cover, contemporaneously during Late Cretaceous/Early Tertiary inversion, (5) major subsidence and salt diapir rise during the Cenozoic. We suggest that the heterogeneity in distribution and timing of deformation in the working area was controlled by pre-existing faults and variations in salt thickness, which led to stress perturbations and therefore local strain partitioning. We observed coupling and decoupling between pre- and post-Zechstein salt units: in decoupled areas deformation occurred only within post-salt units, whereas in coupled areas deformation occurred in both post-salt and pre-salt units and is characterised by strike-slip faulting.

In **chapter 3** 3D retro-deformation was performed on a detailed interpreted 3D structural model to simulate strain in the hanging wall at the time of faulting, at a scale below the seismic resolution. The modelling is based on a clear definition of a 6 km long fault in 3D, and the temporal and kinematic understanding of its deformation. The results show that (1) considerable strain ranging in magnitude between 0% and 20% is observed more than 1 km away from the fault trace, and (2) deformation around the fault causes strain variations, depending on the fault morphology. The angle between the regional and the local strain axis can differ up to 90°. This strain variation is responsible for the heterogeneous sub-seismic fracture distribution observed in wells. We linked the fracture density from well data with the modelled strain magnitude, and used the strain magnitude as a proxy for fracture density. With this method we can predict the relative density of small-scale fractures in areas without well data. Furthermore, knowing the orientation of the local strain axis we predict fault strike, and opening or reactivation of fractures during a particular deformation event. The here suggested workflow is a helpful tool for the prediction of small-scale faults and fractures, which is subsequently important for identifying compartmentalisation and fracture networks, and for improvement of fluid flow simulations and well placement.

In **chapter 4** we demonstrate a fault-analysis of a ca. 13 km long segmented fault, derived from detailed interpretation of a high-resolution 3D seismic data set. Here, we present the evolution of fault-segmentation on one single normal fault, with the combined methods of morphology analysis (dip, azimuth, and curvature attributes) and displacement measurements. We identified four orders of segments on two horizons getting younger with increasing fault-length, over several scales from 200 m to 15000 m fault length. Fault attribute maps (dip, azimuth, curvature) and displacement diagrams emphasise changes on the fault-surface. Our analysis shows a strong variation in slip, throw, and heave, especially in areas where fault-segments are linked. The difference in the amount of displacement increases with undulation along fault-strike and fault-dip. Consequently, throw and heave should not be used as approximations for slip, and are not representative for fault-analysis (e.g. fault-propagation through time, length vs. displacement relationship, displacement vs. cumulative frequency) of large segmented faults. Otherwise, high amounts of slip will be under-represented.

Fault-morphology analyses of large-scale faults can be important for improvement of seismic hazard assessments, as the fault-roughness is possibly associated with the heterogeneous distribution of earthquakes. The here presented slip profiles are characterised by a triangular to half-elliptical shape, rather than being elliptical as proposed in previous studies from 2D seismic data. We assume that the use of 2D profiles instead of 3D data, and the use of heave and throw instead of slip, leads to an incomplete identification of fault-segments, and therefore results not only in a smoothing of the curves, but also in a change from triangular to (half-) elliptical displacement curves. Hence, the high complexity of fault-growth in time and space requires a detailed analysis in 3D.

In **chapter 5** we simulate extensional deformation with scaled physical analogue models using a cohesive mixture of sand and gypsum. The observed structures in the analogue experiments are comparable with the structures recognised in the 3D seismic data set. Also, the fault-growth processes derived from the analogue modelling are comparable to those which underlie the seismic structures in our working area. The experiments were carried out over a large scale range that corresponds to 10 m to 9000 m in nature. The chosen short time window and low displacement rate resulted in a very high spatial (9 pixel/mm) and temporal (1 image every 0.04 mm vertical displacement) resolution. Hence, it was possible for the first time to detect significant deformation processes such as small-scale deformation, initiation and propagation of tensile and shear fractures, vertical linkage of fault-segments, and alternation of fault activity between different faults through time.

In **chapter 6,** a new method for paleostress analysis is introduced. Numerous normal fault-surfaces have been interpreted from the 3D seismic data, and their undulations are analysed in 3D. The axes of corrugations are used as movement directions since they require least energy and therefore smallest strain. Paleostress analysis for the Permian results in a WSW-ENE extension direction, and indicates plain strain deformation. The here for the first time presented stress data derived from 3D seismic data for subsurface Permian strata within the North German Basin, are an important contribution not only methodologically, but also for paleostress analysis within the Southern Permian Basin in general.

In these sub-projects we started studying the heterogeneity in time and distribution in space of large-scale basin-wide structures (chapter 2), continued an order of magnitude lower and focused on the undulation of fault-surfaces (chapters 3, 4, and 6), reaching down to the heterogeneous fracture pattern of small-scale bore-hole data (chapter 4), and finally summing up with the heterogeneous strain evolution in space and time covering a broad scale range with analogue modelling (chapter 5).

At all scales we observed a similar heterogeneity of deformation patterns, but the reasons are different depending on processes relevant for the actual scale (Fig. 7.1). At the large 2D or 3D seismic scale (10^5 to 10^3 m-scale) inherited basement structures, reactivated faults, the position of detachment levels, as well as diapir structures and their growth through time, strongly influence further deformational events by stress field perturbations and subsequent strain partitioning. At a smaller scale (10^2 to 10^1 m-scale), extensional faults are observable as highly undulating surfaces rather than planar faults, which is mainly caused by the growth and finally linkage of numerous smaller fault-segments over time. Movement along these undulating surfaces and the associated displacement changes along fault-strike cause a strong fracturing within the surrounding rocks in a sub-seismic scale (10^1 to 10^{-2} m-scale). In well data this deformation (plus other parameters influencing fracture-generation like rock-anisotropy and fluid pressure) can be identified as apparently chaotic fracture orientation. Alternation of activity between different faults and the thereby occurring propagation of strain through the rock volume appears to be a process which affects all scales.

This high spatial and temporal complexity of deformation can only be understood by the interpretation and analysis of four-dimensional data. Without information about the third or fourth dimension, and without appropriate information about deformation throughout the scale limits, one has to be aware that the scale-range that is investigated is limiting the interpretive potential, and influences the interpreted results as they depend finally on the methodology.

The comparison and correlation of deformation over such a large scale range is a challenge we focused in this project. As far as it is studied in this thesis, deformation can have a similar pattern over large scale ranges, but it often underlies different spatiotemporal causes, and that rises the question of its real correlative nature.

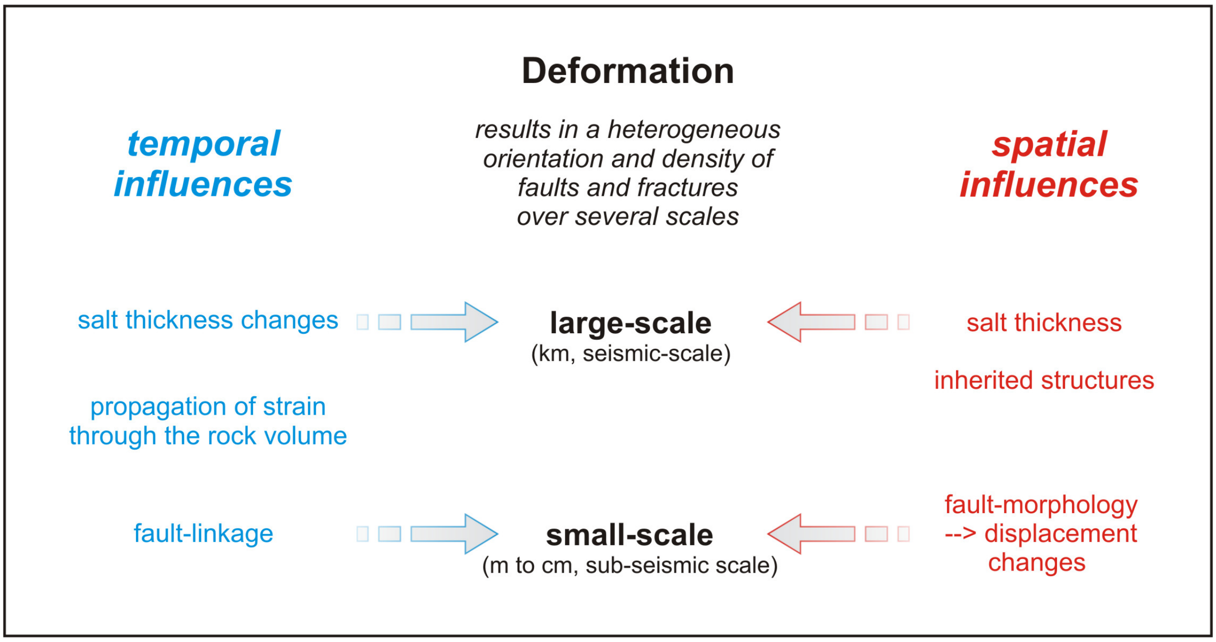

Figure 7.1: Schema illustrating possible tectonic causes for the heterogeneous strain distribution over different scales during one deformation event, as derived from the here presented study within the NW German Basin.